A System of Protein Target Sequences for Anti-RNA-viral Chemotherapy by a Vitamin B$_6$-Derived Zinc-Chelating Trioxa-adamantane-triol

Andreas J. Kesel*

Chammünsterstr. 47, D-81827 München, Germany

Abstract—The synthesis of the structurally unusual heterotricyclic compound 1-[3-hydroxy-5-(hydroxymethyl)-2-methyl-4-pyridinyl]-2,8,9-trioxaadamantane-3,5,7-triol (trivially named bananin, BN) from pyridoxylidenephloroglucinol and a theoretical prospect on possible biological activities of BN are presented in this report. Pyridoxylidenephloroglucinol is synthesized by *Knoevenagel* condensation of the vitamin B$_6$ aldehyde pyridoxal with phloroglucinol. Pyridoxylidenephloroglucinol rearranges to light-yellow (4′*RS*)-1′,4′-dihydrobananin by refluxing in 5 M hydrochloric acid. Air oxidation subsequently forms BN in the heat which immediately yields orange-yellow (4′*RS*)-4′-chloro-1′,4′-dihydrobananin by 1,4-addition of hydrogen chloride. This intermediate could be isolated but, interestingly, not a BN hydrochloride. Brown BN is finally achieved by base-catalyzed elimination of hydrogen chloride from (4′*RS*)-4′-chloro-1′,4′-dihydrobananin. Regarding possible biological activities, it was demonstrated that BN acts as zinc (Zn^{2+}) chelator. Therefore, a target of interest could be the human immunodeficiency virus type 1 (HIV-1) zinc finger HIV-1 RNA-binding nucleocapsid protein p7 (NCp7). Through suggested zinc ejection from HIV-1 genomic RNA ψ-element-binding and HIV-1–RNA-duplex packaging NCp7 by BN, thus rendering NCp7 functionally obsolete, it is deduced that HIV-1 replication and effective infectious virion encapsidation could be inhibited by BN. Furthermore, theoretical and structural considerations propose that BN is converted into bananin 5′-monophosphate (BNP) by the cell type-ubiquitous human enzyme pyridoxal kinase (EC 2.7.1.35). Together with the putative antilentiviral retinoid vitamin A–vitamin B$_6$ conjugate analogue B6RA (Kesel, A. J. *Biochem. Biophys. Res. Comm.* 2003, *300*, 793), BNP is postulated to serve as effector in a system of protein target sequences RX(D/E) of RNA virus components. Human immunodeficiency *Retroviridae* (HIVs) could possibly be influenced by B6RA and BNP. In addition, candidate targets of B6RA and BNP could be adsorption, transcription and/or viral RNA replication of an interestingly wide RNA virus selection including *Picornaviridae* (poliovirus, human coxsackievirus, hepatitis A virus), *Flaviviridae* (yellow fever virus, Dengue virus, West Nile virus, Kunjin virus, St. Louis encephalitis virus, hepatitis C virus), *Togaviridae* (rubella virus), *Coronaviridae* (human coronavirus, human SARS-associated coronavirus), *Rhabdoviridae* (rabies virus), *Paramyxoviridae* (human parainfluenza virus, measles virus, human respiratory syncytial virus), *Filoviridae* (Marburg virus, Ebola virus), *Bornaviridae* (Borna disease virus), *Bunyaviridae* (Hantaan virus), *Arenaviridae* (Lassa virus), and *Reoviridae* (human rotavirus). The postulated scope of 'metabolically trapped' BNP might resemble the antiviral spectrum of the RNA-viral virustatic ribavirin.
© 2003 Elsevier Ltd. All rights reserved.

Introduction

Oligo-oxa-adamantanes are rarely found in nature as structurally striking biochemicals. The neurotoxic sodium channel blocker tetrodotoxin (TTX), one of the most toxic non-proteinaceous poisons along with aconitine, veratridine, saxitoxin (STX), batrachotoxin (BTX) and palytoxin (PTX), is widely spread in nature, especially in marine ecosystems. TTX, traditionally esteemed famous for its occurrence in the inner organs (especially liver and ovaries) of the Japanese culinaric delicacy *tora fugu*, the globe (tiger puffer) fish *Spheroides rubripes* (*Tetraodontidae*), is to be depicted as substituted 2,8-dioxa-adamantane[1] (Fig. 1).[1−3] Daigremontianin was isolated from the tropical flower *Kalanchoe daigremontiana* Hamet *et* Perr. (*Crassulaceae*) and was shown to be a steroid (bufadienolide) 2,8,9-trioxa-adamantane (Fig. 1).[4,5] Synthetic adamantanes, or tricyclo[3.3.1.1^{3,7}]decanes, are used as antiviral chemotherapeutics [amantadine (1-amino-adamantane)

*Corresponding author. Tel.:+49-89-453-64500; fax:+49-89-453-64501; e-mail: andreas.kesel@t-online.de

and rimantadine systemically against influenza A virus, tromantadine topically against herpes simplex virus type 1 infections] and antiparkinsonian (muscle relaxant) drugs [amantadine as central dopaminergic, memantine (1-amino-3,5-dimethyl-adamantane) as neuroprotective *N*-methyl-D-aspartate (NMDA)-subtype glutamate receptor antagonist] (Fig. 1).

In addition to the *Schiff* base[6] formation of pyridoxal (mainly existing as racemic cyclic hemiacetal, especially as hydrochloride) and pyridoxal 5′-phosphate (coenzyme vitamin B$_6$) with primary amino groups of biomolecules which is of central importance in coenzyme vitamin B$_6$-catalyzed biochemical metabolism (transamination, decarboxylation, racemization, ligation, lysis) of amino acid, neurotransmitter, phospholipid, sphingolipid, heme, polyamine and tumor marker[7] synthesis, pyridoxal and pyridoxal 5′-phosphate are capable of undergoing various chemical reactions. Especially *Knoevenagel* condensations lead to interesting compounds with antiretroviral, oncolytic, immunosuppressant, antioxidative, free radical-scavenging, nitric oxide synthase inhibition and other biological activities.[8–12] Recently, a new conception for inducing selective apoptosis in human immunodeficiency virus

type 1 (HIV-1)-infected cells was proposed.[12] Therefore, my attention focused on the analysis of unique reactions of vitamin B$_6$ which was shown to be suitable for various chemical transactions.[8–12]
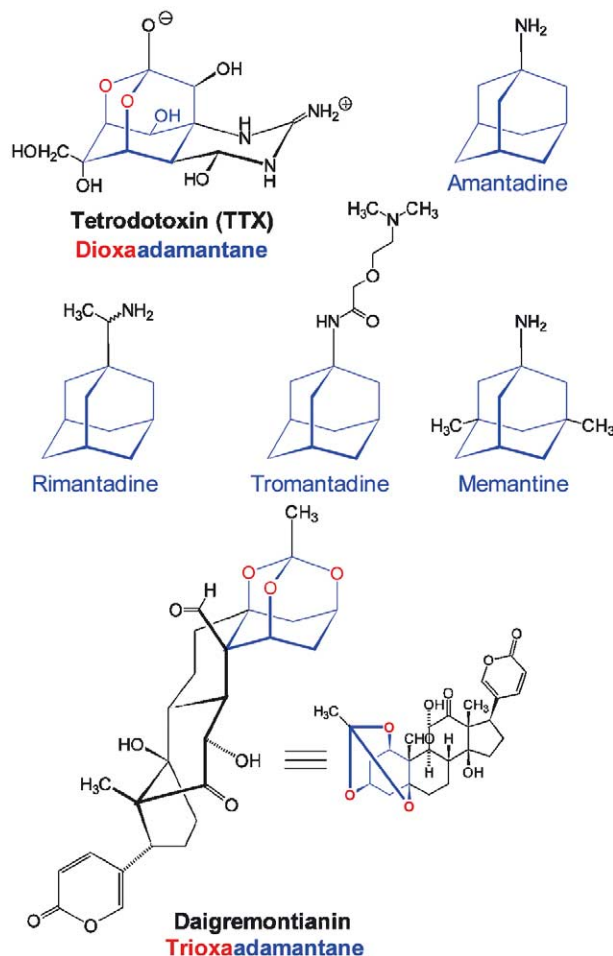
Results and Discussion

Infrared absorption spectroscopy of the reaction product resulting from the heat and hydrochloric acid treatment of pyridoxylidenephloroglucinol

An infrared absorption (IR) spectrum of the reaction product was recorded in a solid potassium bromide (KBr) pellet (Fig. 2). No α,β-unsaturated, quinoid carbonyl absorption at wavenumbers between 1700 and 1600 cm^{-1} could be seen. Instead a very broad OH band between 3650 and 1800 cm^{-1} dominates the IR spectrum. It represents a valence bond vibration of hydrogen-bonded O–H, and, respectively, intra/intermolecular polymeric associated chelate O–H. At 2900 cm^{-1} a methyl group C–H and at 2825 cm^{-1} a methylene group C–H valence bond vibration can be identified. At 1590 and 1520 cm^{-1} C–C aromatic valence bond vibrations of a pyridine heterocycle can be detected. At wavenumbers of 1430 cm^{-1} a methylene C–H deformation vibration and 1395 cm^{-1} a methyl group C–H deformation vibration can be analyzed. Very characteristic is the aromatic C–O phenolic valence bond vibration at 1210 cm^{-1}. The two bands at 1065 cm^{-1} (Ar–CH$_2$–OH) and 1110 cm^{-1} are aliphatic C–O valence bond vibrations. The absorption band at 820 cm^{-1} is fitting to a 1,2,3,4-tetrasubstituted aromate with one isolated CH. Taken together, already the IR data unequivocally proof the unusual 1-[3-hydroxy-5-(hydroxymethyl)-2-methyl-4-pyridinyl]-2,8,9-trioxaadamantane-3,5,7-triol structure because the 6-hydroxy-4-(hydroxymethyl)-1-methyl-8*H*-[1]benzopyrano[2,3-c]pyridin-8-one alternative would have a strong α,β-unsaturated, quinoid carbonyl absorption between wavenumbers of 1775 and 1650 cm^{-1} (preferably 1650–1700 cm^{-1}, *p*-benzoquinone 1669 cm^{-1}). The predominant, very broad OH band from 3650 to 1800 cm^{-1} peaking at 3350 cm^{-1} pointed to strongly associated intermolecular hydrogen bonds in the solid state of the brown substance KBr pellet. A similar effect was observed in the IR spectrum (in KBr) of the polyhydroxyl, solvent-retaining compound tetrodotoxin.[3]

UV spectrophotometry of the reaction product resulting from the heat and hydrochloric acid treatment of pyridoxylidenephloroglucinol
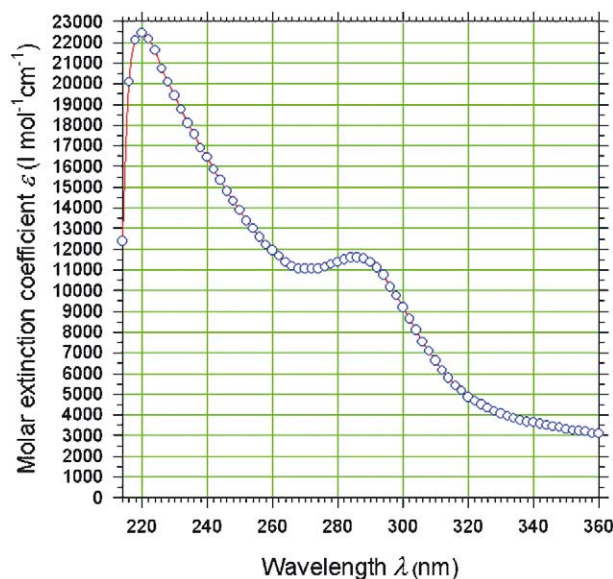
An UV electronic absorption spectrum of the substance was recorded in 0.1 M sodium hydroxide solution (Fig. 3). The solubility of the material in water, ethanol, or dilute acid [dilute hydrochloric (HCl) and sulfuric acid (H$_2$SO$_4$)] is too low to work in these solvents. The product is soluble in sodium hydroxide solution and dimethyl sulfoxide (DMSO) to give yellow to brown solutions. The UV spectrum showed two maxima at 220.0 nm (ε = 22,443 L mol^{-1} cm^{-1}) and 285.8 nm (ε = 11,591 L mol^{-1} cm^{-1}), the molar mass for the cal-

Figure 1. The natural products tetrodotoxin and daigremontianin with oligo-oxa-adamantane structure and the synthetic adamantanes, or tricyclo[3.3.1.1^{3,7}]decanes, amantadine, rimantadine, tromantadine, and memantine.
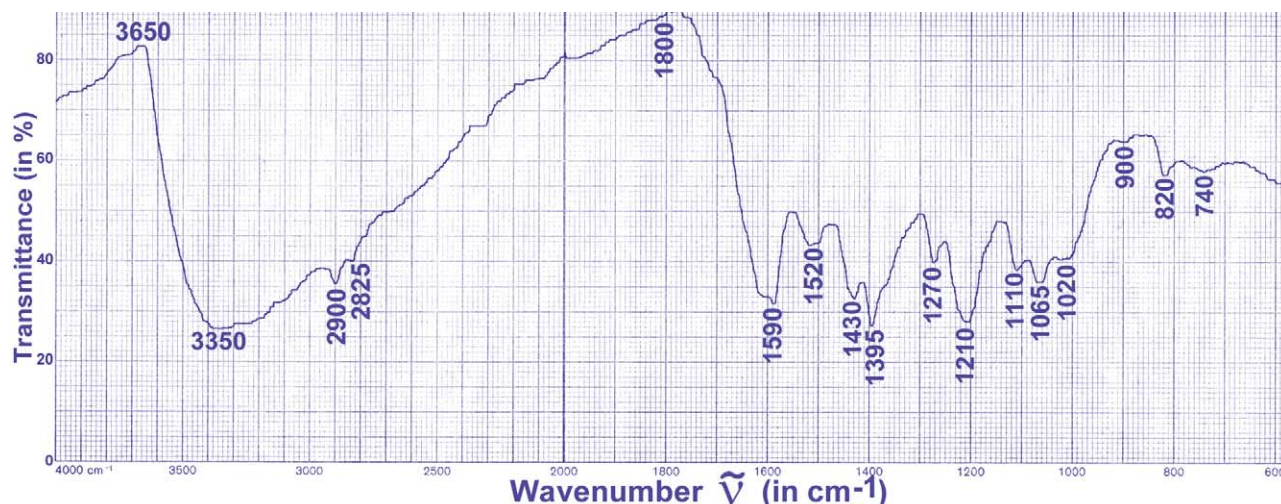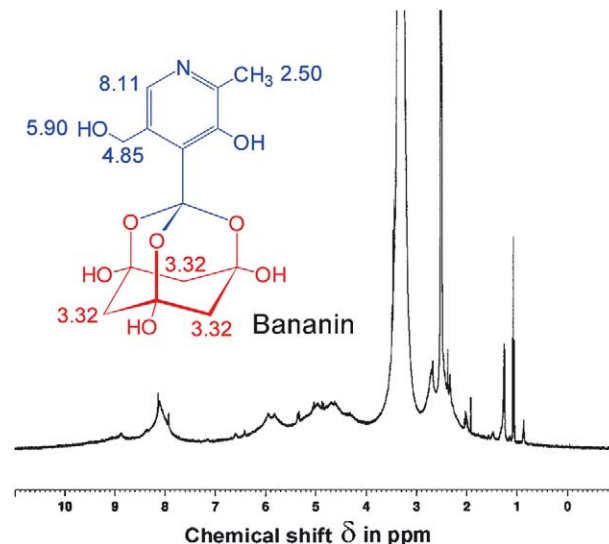
Figure 2. Infrared (IR) absorption spectrum measured in potassium bromide (KBr) solid disc of the unknown brown-black reaction product resulting from the heat and hydrochloric acid treatment of pyridoxylidenephloroglucinol.

Figure 3. UV electronic absorption spectrophotometry of the unknown brown-black reaction product resulting from the heat and hydrochloric acid treatment of pyridoxylidenephloroglucinol. For this purpose, 0.70 mg substance were dissolved in an 100.00 mL volume of 0.1 M sodium hydroxide (NaOH) solution. The maximal absorption of the yellow solution stayed in the linear range of the spectrophotometer ($A < 0.8$).

Figure 4. ^{1}H NMR spectrum of bananin in CDCl$_3$. The bananin contained as impurities the synthesis solvents ethanol [δ 1.18 (t), 3.59 (q)] and water [in CDCl$_3$ δ 1.28 (s)]. Additionally, traces of the synthesis educt pyridoxylidenephloroglucinol [δ 2.70 (s, CH_3), 5.37 (d, CH_2OH), 6.42 (s, HO–C=CH–C=O), 6.60 (s, HO–C=CH–C=O), 7.13 (s, arCH=R), 8.89 (s, pyridine CH)] were detectable.

culation of the molar extinction coefficient ε was choosed as $M = 327.29$ g/mol, the theoretic molar mass of 1-[3-hydroxy-5-(hydroxymethyl)-2-methyl-4-pyridinyl]-2,8,9-trioxaadamantane-3,5,7-triol (Fig. 3). This result can be reasonably interpreted in the way that a typical sodium phenolate [sodium phenolate in water: $\lambda_{1,max} = 235$ nm ($\varepsilon = 9400$), $\lambda_{2,max} = 287$ nm ($\varepsilon = 2600$)] is the chromophor of the compound. The structure 6-hydroxy-4-(hydroxymethyl)-1-methyl-8H-[1]benzopyrano[2,3-c]pyridin-8-one would show an electronic absorption maximum at a wavelength of approximately 450 nm similar to the α,β-unsaturated carbonyl condensate B6PR.[11] Therefore, the UV spectrophotometry supplies us with strong evidence for 1-[3-hydroxy-5-(hydroxymethyl)-2-methyl-4-pyridinyl]-2,8,9-trioxaada-

mantane-3,5,7-triol to represent the UV chromophor of the unknown product. Already now the spectral-analytic structure determination provides growing proof for being 1-[3-hydroxy-5-(hydroxymethyl)-2-methyl-4-pyridinyl]-2,8,9-trioxatricyclo[3.3.1.1^{3,7}]decane-3,5,7-triol the suspected structural composition of the material in question.

Proton nuclear magnetic resonance (^{1}H NMR) spectroscopy of the reaction product resulting from the heat and hydrochloric acid treatment of pyridoxylidenephloroglucinol

The final structural proof could be made by examination of the ^{1}H NMR spectrum of the substance in deuterated chloroform (CDCl$_3$) (Fig. 4). At the chemical shift δ 2.50 a singlet of three protons of the
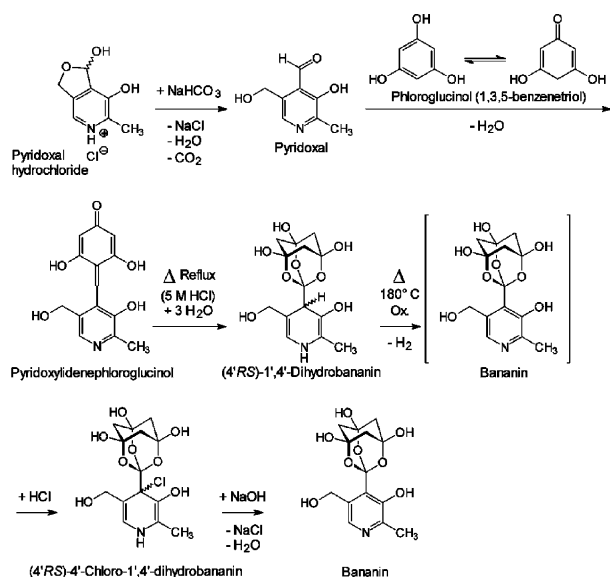
Figure 5. Chemical synthesis of 1-[3-hydroxy-5-(hydroxymethyl)-2-methyl-4-pyridinyl]-2,8,9-trioxaadamantane-3,5,7-triol. The *Knoevenagel* condensation of phloroglucinol and pyridoxal hydrochloride yields pyridoxylidenephloroglucinol. Its heat treatment with 5 M hydrochloric acid firstly produces light yellow (4'*RS*)-1',4'-dihydrobananin. Subsequently air oxidation in the heat precipitates the orange-yellow (4'*RS*)-4'-chloro-1',4'-dihydrobananin which results from addition of hydrogen chloride to bananin. (4'*RS*)-4'-chloro-1',4'-dihydrobananin eliminates hydrogen chloride by treatment with strong bases (NaOH). Finally, the brown-black bananin is isolated by help of its relative insolubility in water.

heteroaromatic methyl group peaked. At δ 3.32 six protons of the methylene groupings of the trioxa-adamantane-triol could be unequivocally identified. At δ 4.85 (m, 2H, pyridine C*H*₂OH) and δ 5.90 (m, 1H, CH₂O*H*) the intermolecular-associated hydroxymethyl group gave broadened multiplets emerging possibly from interaromatic charge-transfer complexation and hydrogen-bonding. At δ 8.11 one heteroaromatic proton proofed to complete that no other structural composition was possible than 1-[3-hydroxy-5-(hydroxymethyl) - 2 - methyl - 4 - pyridinyl] - 2,8,9 - trioxatricyclo[3.3.1.1³,⁷]decane-3,5,7-triol. Ethanol, water, and the educt pyridoxylidenephloroglucinol were detectable as trace impurities from synthesis.

Conclusion

Structural, supramolecular and physicochemical aspects of BN

Since the organic chemical structure of the material resulting from the heat and hydrochloric acid treatment of pyridoxylidenephloroglucinol could be defined by the analytical results, an experimentally based scheme for the chemical reactions leading to the synthesis of 1-[3-hydroxy-5-(hydroxymethyl)-2-methyl-4-pyridinyl]-2,8,9-trioxatricyclo[3.3.1.1³,⁷]decane-3,5,7-triol is depicted (Fig. 5). The hypothesis that bananin is an highly intermolecular-associated material, leading to a nearly black colour through interaromatic charge-transfer complexation between the pyridine heterocycles and hydro-
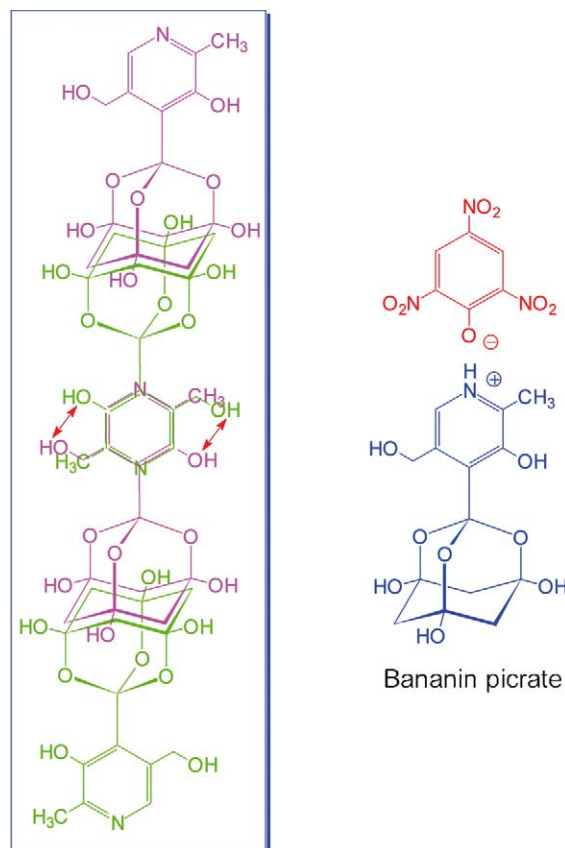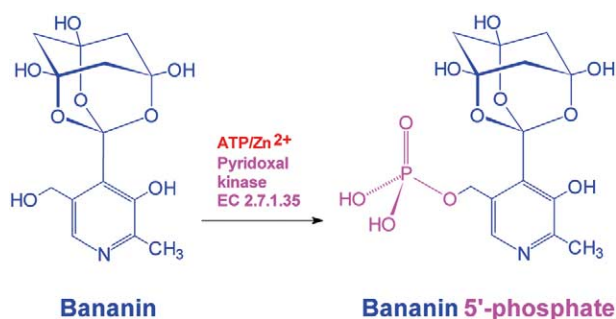

Figure 6. Left, excerpt of the intermolecular association of black bananin leading to supramolecular chains including charge-transfer complexes between the aromatic rings and strong hydrogen-bonding between OH groups (red arrows) and the trioxa-adamantane-triol cages (magenta-green). Right, chemical structure of the yellow bananin picrate.

gen-bonding between the trioxa-adamantane-triol heterotricycles is supported by combination of the IR, UV, and ¹H NMR data (Fig. 6). An instruction protocol for the isolation of amorphous bananin picrate was developed. Amorphous bananin picrate is soluble in water with intense yellow colour and liberates brown-black amorphous bananin by treatment with strong bases (NaOH solution). The intermolecular network leading to the black colour of bananin is interrupted in the yellow bananin picrate (Fig. 6) by complexing the pyridine heterocycle with picric acid. Furthermore, a sodium hydroxide-containing solution of bananin monosodium salt in water both forms a blue copper complex with Cu(OH)₂ and a white zinc complex with Zn(OH)₂. It is proposed that bananin behaves as bidentate chelate donor to build the tetragonal-planar coordination complex (*SP-4-1*)-bis[1-[3-hydroxy-5-(hydroxymethyl) - 2 - methyl - 4 - pyridinyl] - 2,8,9 - trioxaadamantane-3,5,7-triolato(1-)-*O²,O³'*]copper (Fig. 7) and the tetrahedral coordination complex (*T-4*)-bis[1-[3-hydroxy-5-(hydroxymethyl)-2-methyl-4-pyridinyl]-2,8,9-trioxaadamantane-3,5,7-triolato(1-)-*O²,O³'*]zinc (Fig. 7). In addition, it should be mentioned that bananin has lost most of its vitamin B₆ character. The pyridine nitrogen is less basic than in pyridoxal and the UV parameters of pyridoxine/pyridoxal are left. Instead a typical phenolic behaviour is found and the tendency of
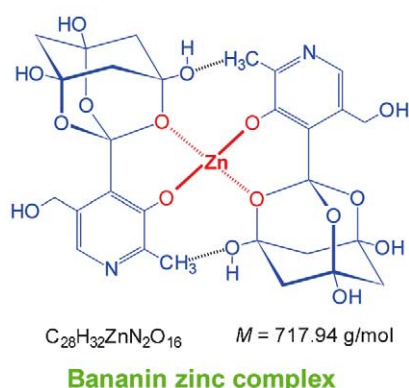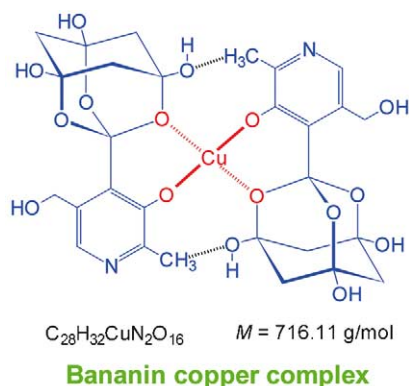
Figure 7. Proposed chemical composition of the cupric complex of bananin, the tetragonal-planar bidentate chelate (*SP-4-1*)-bis[1-[3-hydroxy - 5 - (hydroxymethyl) - 2 - methyl - 4 - pyridinyl] - 2,8,9 - trioxaadamantane-3,5,7-triolato(1-)-$O^2,O^{3'}$]copper [bis(bananinato)copper, bisBNcopper], and the zinc complex of bananin, the presumably tetrahedral bidentate chelate (*T-4*)-bis[1-[3-hydroxy-5-(hydroxymethyl)-2 - methyl - 4 - pyridinyl] - 2,8,9 - trioxaadamantane - 3,5,7 - triolato(1 -) - $O^2,O^{3'}$]zinc [bis(bananinato)zinc, bisBNzinc].

Figure 9. Postulated zinc ejection from HIV-1 (isolate HXB2) RNA-binding NCp7 holoprotein zinc finger sequence motifs I and II (yellow: L-cysteine, black: conserved hydrophobic L-amino acids, magenta: coordinatively Zn^{2+} -bound L-histidine moieties) by four BN to yield defunctional NCp7 apoprotein, devoid of two Zn^{2+} cations, and two bisBNzinc.
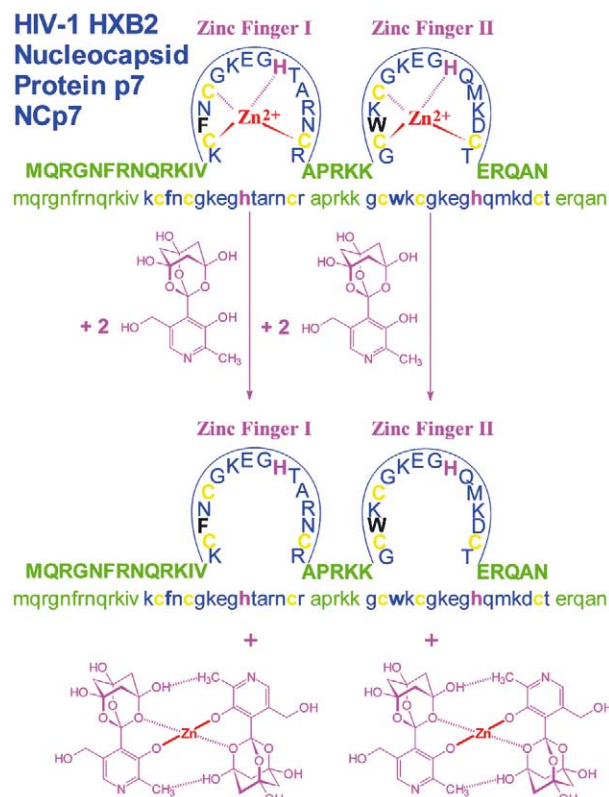

Figure 8. Enzymatic intracellular phosphorylation of BN to BNP by human pyridoxal kinase resulting in 'metabolic trapping' of BNP inside the cell.

vitamin B_6 to exist mostly in a well-defined zwitterionic state at physiologic pH 7.4 is abandoned in bananin.

Intracellular enzymatic phosphorylation of BN to BNP by human pyridoxal kinase

To move a step toward the direction of possible biological activities of BN it is suggested that human pyridoxal kinase[13] accepts BN as a substrate for ATP- and Zn^{2+}-dependent phosphorylation to bananin 5′-phosphate (BNP) (Fig. 8). Pyridoxal kinase can phosphorylate an array of vitamin B_6-derivatives with modulated substituents in position 4 of the pyridine heterocycle, additionally to its natural substrates pyridoxine, pyridoxal and pyridoxamine.[14,15] This was theoretically proofed by the crystal structure determination of sheep brain pyridoxal kinase[16] which shows a tight binding of the 3 - hydroxy - 5 - (hydroxymethyl) - 2 - methylpyridine vitamin B_6 core structure of pyridoxal in the substrate-binding pocket, but structural fill space at the 4-position of the vitamin B_6 core element.[16] Conclusively, it is reasonable to speculate that BN is converted into BNP by the human tissue-ubiquitous pyridoxal kinase,[13] and such is 'metabolically trapped' inside the cell after cellular uptake by vitamin B_6 carrier systems. Through usage of vitamin B_6 metabolic systems high intracellular concentrations of BNP could be achieved since the phosphate group-induced zwitterionic, hydrophilic appearance of BNP prevents reverse cell membrane passage.

Biological significance of zinc complexation by BN for zinc ejection from HIV-1 nucleocapsid protein NCp7

The HIV-1 *gag* gene polycistronic mRNA product encodes the myristoylated matrix protein p17, the
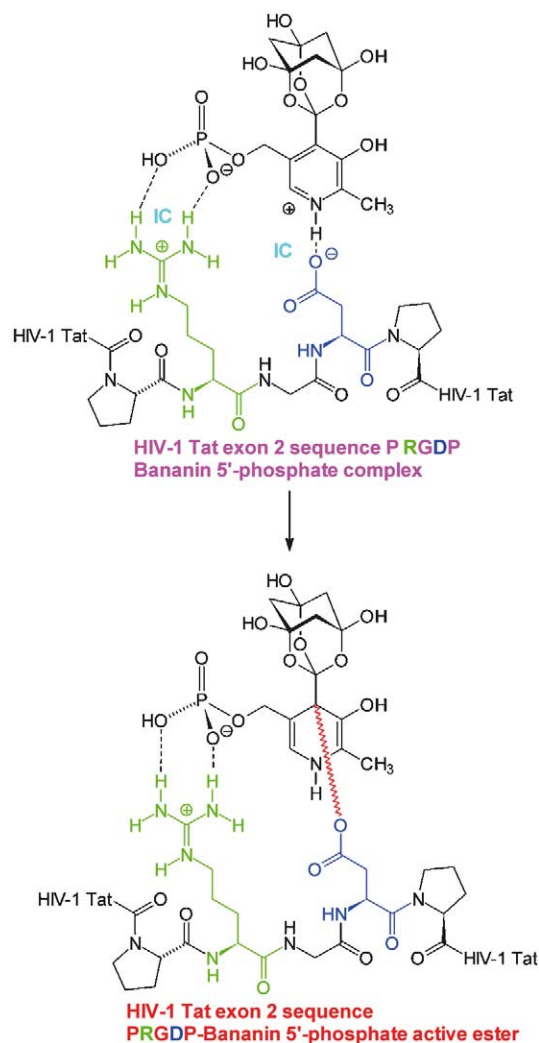
Figure 10. Example of a proposed covalent active ester formation of BNP at a selected, representative RNA-viral, HIV-1 *trans*-activating transcriptional regulatory Tat protein RGD sequence (see Table 1) by addition of the aspartate group to the pyridine ring of RGD-ionic contact (IC)-bound BNP resulting in an activated 1,4-dihydro-4-pyridinyl ester.

Proposed active ester formation of BNP at selected RNA-viral protein RX(D/E) target sequences

In analogy to the postulated antiviral mechanism of the retinoid vitamin A-vitamin B_6 conjugate analogue B6RA at RGD and RLE viral protein target sequences,[12] a covalent 1,4-dihydro-4-pyridinyl active ester formation of BNP with RGD aspartic acid residues in RNA-viral protein target sequences is proposed (Fig. 10). BNP should have a similar salt-bridge amphoteric affinity to RX(D/E) protein sequence motifs like B6RA. Therefore, it could covalently bind to viral RX(D/E) sequences and, analogously to B6RA, chemically modify important viral proteins, thus making them functionally obsolete. Together with the putative antilentiviral retinoid vitamin A–vitamin B_6 conjugate analogue B6RA, BNP is proposed to serve as effector in a system of protein target sequences RX(D/E) of RNA virus components. Human immunodeficiency virus type 1 (HIV-1) *trans*-activating transcriptional regulatory protein Tat sequences PRGDP and PRLEP were suggested as possible targets of B6RA.[12] I propose a binding of B6RA/BNP to Tat PRGDP *tat* exon 2-encoded C-terminal sequence which serves also for cross-talk with cellular tumor suppressor protein p53.[12] BNP could form an active ester at the *tat* exon 2-encoded C-terminal PRGDP sequence (Fig. 10) by addition of the aspartate (D) residue to the trioxa-adamantane-triol 4-substituent-activated pyridine heterocycle in BNP (Fig. 10). This 1,4-dihydro-4-pyridinyl active ester species would be principally able to cross-link Tat D-amide-like to amino groups of DNA nucleobases (adenine, guanine, cytosine) in HIV-1 proviral integrated U3/R sequences of HIV-1 5′-long terminal repeat or, more generally, in host cellular DNA. In this way, non-repairable Tat protein–DNA complexes would serve as trigger for DNA damage-induced apoptosis selectively in cells in which Tat is present. As a result the host organism would be specifically extricated from integrated HIV-1 proviruses.[12] A database search[36] and most recent status Medline/PubMed search[37] for RGD-similar sequences was performed for human RNA viruses (Table 1). The most important human RNA virus pathogens were considered. Surprisingly, many indispensable virus proteins contain often conserved B6RA- and BNP-binding triplets RX(D/E) which are frequently surrounded by hydrophobic protein sequence strips enhancing affinity for the B6RA hydrophobic vitamin A chain (Table 1). Candidate targets of B6RA and BNP were found within proteins of RNA viruses like *Picornaviridae* (poliovirus, human coxsackievirus, hepatitis A virus), *Flaviviridae* (yellow fever virus, Dengue virus, West Nile virus, Kunjin virus, St. Louis encephalitis virus, hepatitis C virus), *Togaviridae* (rubella virus), *Coronaviridae* (human coronavirus, human SARS-associated coronavirus), *Rhabdoviridae* (rabies virus), *Paramyxoviridae* (human parainfluenza virus, measles virus, human respiratory syncytial virus), *Filoviridae* (Marburg virus, Ebola virus), *Bornaviridae* (Borna disease virus), *Bunyaviridae* (Hantaan virus), *Arenaviridae* (Lassa virus), *Reoviridae* (human rotavirus), and *Retroviridae* (HIV-1). The antiviral scope of B6RA/BNP may be related to the broad-spectrum

phosphorylated p24 core protein, the small core peptide p2, the zinc-containing nucleocapsid protein NCp7, the small core peptide p1, and the virion-incorporated core link protein p6. NCp7 contains two highly conserved nonclassical Cys-Xaa$_2$-Cys-Xaa$_4$-His-Xaa$_4$-Cys (CCHC) zinc finger motifs.[17−35] This retroviral zinc finger motif is conserved in all onco- and lentiretroviruses except spumaretroviruses.[23] NCp7 binds to the duplex of HIV-1 retrogenomic mRNA encapsidated in the mature virion core at the highly secondary-structured HIV-1 RNA sequence elements known as ψ-packaging signal near the 5′-LTR, next to the tRNA^{Lys} primer binding (PB) site. The two zinc fingers are sensitive to organic-chemical zinc chelating compounds. 3-Nitrosobenzamide (NOBA)[17−19] and other small molecule compounds[25−28,31−33,35] eject zinc from NCp7 holoprotein leaving a functionally deprived apoprotein. Therefore, zinc chelators are able to inhibit HIV-1 replication and infectivity in vitro[17−19,21,23] and in vivo.[34] BN is an excellent zinc chelator and is postulated to be chemically suitable for zinc ejection from HIV-1 NCp7 (Fig. 9).

anti-RNA-viral virustatic ribavirin[38] because ribavirin is mostly active against RNA viruses by inhibiting inosine 5′-monophosphate dehydrogenase as ribavirin 5′-monophosphate, and mRNA precursor 5′-capping as ribavirin 5′-triphosphate.[38] The actual therapeutic value of the B6RA/BNP system for chemotherapeutic treatment of RNA-viral human disease conditions remains elusive until comprehensive experimental verification is gained.

Experimental

Synthesis of pyridoxylidenephloroglucinol from pyridoxal hydrochloride and phloroglucinol

A mass of 20.81 g pyridoxal hydrochloride ($M = 203.63$ g/mol) ($n = 102.1952$ mmol) was dissolved in 63 mL water by heating on a water bath. 12.89 g phloroglucinol ($M = 126.11$ g/mol) ($n = 102.2123$ mmol) were dissolved in 79 mL of ethanol 90% by heating on a water bath. The two solutions were mixed and refluxed for 10 min. Then 8.59 g sodium bicarbonate ($NaHCO_3$) ($M = 84.01$ g/mol) ($n = 102.2497$ mmol) were added to the hot yellow solution. A bright yellow precipitate formed after approximately 10 min on reflux. The suspension was additionally heated for 5 min on a water bath, cooled slowly to room temperature, and freezed to $-18°$ C for 4 h. Then the precipitate was vacuum filtered and transferred and washed with 65 mL water. It was dried over anhydrous calcium chloride ($CaCl_2$) in a vacuum desiccator. Yield: 28.1 g yellow powder (100%) pyridoxylidenephloroglucinol $C_{14}H_{13}NO_5$ ($M = 275.26$ g/mol).

Synthesis of 1-[3-hydroxy-5-(hydroxymethyl)-2-methyl-4-pyridinyl]-2,8,9-trioxaadamantane-3,5,7-triol (bananin) from pyridoxylidenephloroglucinol

28.1 g pyridoxylidenephloroglucinol ($M = 275.26$ g/mol) ($n = 102.0853$ mmol) were suspended in 100 mL of 5 M hydrochloric acid (500 mmol HCl). The dark yellow solution was refluxed for 15 min on a water bath. A caramel-yellow coloured precipitate of 1′,4′-dihydrobananin formed. Then it was heated to 170-180° C on an air bath and the orange-yellow (4′RS)-4′-chloro-1′,4′-dihydrobananin formed in the heat. When the reaction proceeds the heat is reduced to 120° C and then the mixture was cooled slowly to room temperature. Then it was freezed to $-18°$ C for 12 h. The nearly solid orange-yellow suspension was filtered through a paper filter. The yellow-orange residue was suspended in 300 mL saturated (room temperature $\theta = 20°C$) sodium bicarbonate ($NaHCO_3$) solution in water. The orange-yellow (4′RS)-4′-chloro-1′,4′-dihydrobananin eliminated HCl to form bananin. Then solid sodium hydroxide (NaOH) pearls were added in small portions to the suspension until all material had dissolved to form a coffee-black solution ($V = 400$ mL) of bananin sodium salt. It was titrated in small portions with 10 M hydrochloric acid until brown bananin precipitated. The chocolate brown suspension was left standing at room temperature for 3 days. After that time the suspension was fil-

tered through a paper filter and the chocolate brown residue in the filter was washed with 400 mL water. It was dried for 2 weeks over anhydrous calcium chloride ($CaCl_2$) in a vacuum desiccator. Yield: 33.2 g brown-black powder (99%) 1-[3-hydroxy-5-(hydroxymethyl)-2-methyl-4-pyridinyl]-2,8,9-trioxaadamantane-3,5,7-triol (bananin) $C_{14}H_{17}NO_8$ ($M = 327.29$ g/mol). IR (KBr) (wavenumber in cm^{-1}): 3350 (very broad, ν O–H, s), 2900 (ν C–H, CH_3, w), 2825 (ν C–H, CH_2, w), 1590 (ν C=C, pyridine, m), 1520 (ν C=C, pyridine, m), 1430 (δ C–H, CH_2, m), 1395 (δ C–H, CH_3, m), 1270 (ν C–O–C, w), 1210 (ν arC–OH, m), 1110 (ν C–OH, w), 1065 (ν C–O, CH_2OH, w), 1020 (ν C–OH, w), 900 (w), 820 (δ pyridine C–H, w), 740 (δ CH_2, rocking, w). UV (0.1 M NaOH solution): $\lambda_{max,1} = 220.0$ nm [$\varepsilon = 22{,}443$ L mol^{-1} cm^{-1}; A (1%/1 cm) = 686], $\lambda_{max,2} = 285.8$ nm [$\varepsilon = 11{,}591$ L mol^{-1} cm^{-1}; A (1%/1 cm) = 354]. ^1H NMR ($CDCl_3$): δ 2.50 (s, 3H, pyridine CH_3), 3.32 (s, 6H, CH_2), 4.85 (m, 2H, pyridine CH_2OH), 5.90 (m, 1H, CH_2OH), 8.11 (s, 1H, pyridine CH).

Qualitative preparation of amorphous 1-[3-hydroxy-5-(hydroxymethyl) - 2 - methyl - 4 - pyridinyl] - 2,8,9 - trioxaadamantane-3,5,7-triol picrate (amorphous bananin picrate)

A saturated solution (50 mL at 80° C) of 1-[3-hydroxy-5-(hydroxymethyl) - 2 - methyl - 4 - pyridinyl] - 2,8,9 - trioxaadamantane-3,5,7-triol (bananin) in dimethyl sulfoxide (DMSO) was mixed with 50 mL of a saturated (room temperature $\theta = 20°C$) solution of picric acid (2,4,6-trinitrophenol) in 50% ethanol. Then 200 mL 90% ethanol and 500 mL water were added in the heat. A voluminous yellow precipitate formed. The temperature of the suspension was kept at $-18°C$ for 12 h. The precipitate was vacuum filtered and dried over anhydrous calcium chloride ($CaCl_2$) in a vacuum desiccator. Yield: yellow powder of crude (bananin-containing) 1-[3-hydroxy-5-(hydroxymethyl)-2-methyl-4-pyridinyl]-2,8,9-trioxaadamantane-3,5,7-triol picrate (bananin picrate). Purification: the crude product was dissolved in 200 mL 5 M hydrochloric acid (1 mol HCl) by heating on a water bath and the mixture was hot filtrated. In the filter residual brown-black bananin remained. The filtrate was slowly neutralized with a solution of 40.0 g sodium hydroxide (1 mol NaOH) in 200 mL water. Yellow bananin picrate precipitated. The precipitate was vacuum filtered and dried over anhydrous calcium chloride ($CaCl_2$) in a vacuum desiccator. Yield: yellow amorphous powder 1-[3-hydroxy-5-(hydroxymethyl)-2-methyl-4-pyridinyl]-2,8,9-trioxaadamantane-3,5,7-triol picrate (bananin picrate).

Qualitative preparation of amorphous (SP-4-1)-bis[1-[3-hydroxy-5-(hydroxymethyl)-2-methyl-4-pyridinyl]-2,8,9-trioxaadamantane-3,5,7-triolato(1-)-O^2,$O^{3'}$]copper [bananin copper complex, bis(bananinato)copper, bisBNcopper]

Suspension A: a saturated (room temperature $\theta = 20°C$) solution of cupric sulfate pentahydrate ($CuSO_4 \cdot 5H_2O$) in 100 mL of water was mixed with 100 mL of 1 M sodium hydroxide solution. Blue cupric hydroxide

Table 1. Selection of RNA virus B6RA/BNP-affinity protein sequence motifs RX(D/E)

Virus	Virus Family Subfamily Genus	Strain	Virus Protein	B6RA/BNP Target Sequence
Polio type 1	Picornaviridae Enterovirus	Mahoney, Sabin	**3D** RNA-dependent RNA Polymerase	2006-FGD**RVD**YI-2013
Polio type 2	Picornaviridae Enterovirus	Lansing, P712	**3D** RNA-dependent RNA Polymerase	2004-FGD**RVD**YI-2011
Polio type 3	Picornaviridae Enterovirus	Sabin vaccine P3/Leon/37, Sabin vaccine P3/Leon/12a[1]b, 23127	**3D** RNA-dependent RNA Polymerase	2003-FGD**RVD**YI-2010
Polio type 1	Picornaviridae Enterovirus	Mahoney, Sabin	**3D** RNA-dependent RNA Polymerase	2125-FF**RAD**EKYPFLI-2136
Polio type 2	Picornaviridae Enterovirus	Lansing	**3D** RNA-dependent RNA Polymerase	2123-FF**RAD**EKYPFLV-2134
Polio type 3	Picornaviridae Enterovirus	Sabin vaccine P3/Leon/37, Sabin vaccine P3/Leon/12a[1]b, 23127	**3D** RNA-dependent RNA Polymerase	2122-FF**RAD**EKYPFLI-2133
Human Coxsackie A9	Picornaviridae Enterovirus	Griggs	**3D** RNA-dependent RNA Polymerase	2113-FLKRYF**RAD**EQYPFLV-2128
Human Coxsackie A24	Picornaviridae Enterovirus	EH24/70	**3D** RNA-dependent RNA Polymerase	2126-FLKRFF**RAD**EKYPFLV-2141
Human Coxsackie B1	Picornaviridae Enterovirus	Japan	**3D** RNA-dependent RNA Polymerase	2094-FLKRYF**RAD**EQYPFLV-2109
Human Coxsackie B3	Picornaviridae Enterovirus	Nancy	**3D** RNA-dependent RNA Polymerase	2097-FLKRYF**RAD**EQYPFLV-2112

Table 1 (*continued*)

Virus	Virus Family	Strain	Virus Protein	B6RA/BNP
	Subfamily			Target Sequence
	Genus			
Human Coxsackie B4	Picornaviridae Enterovirus	E2, JVB / Benschoten / New York/51	**3D** RNA-dependent RNA Polymerase	2095-FLKRYF**RADE**QYPFLV-2110
Human Coxsackie B5	Picornaviridae Enterovirus	1954/UK/85	**3D** RNA-dependent RNA Polymerase	2097-FLKRYF**RADE**QYPFLV-2112
Human Severe Acute Respiratory Syndrome (SARS) Corona	Coronaviridae Coronavirus	Tor2, CUHK-W1, Urbani	Putative **NSP9** in ORF1ab Polyprotein RNA-dependent RNA Polymerase	4470-FFK**RVD**GDMVP-4481
Human Severe Acute Respiratory Syndrome (SARS) Corona	Coronaviridae Coronavirus	Tor2, CUHK-W1, Urbani	Putative **NSP10** in ORF1ab Polyprotein Metal-binding NTPase Helicase	5634-IIPARA**RVE**CFDKFKV-5649
Rabies	Rhabdoviridae Lyssavirus	Pasteur / PV, SAD B19	**L** RNA-directed RNA Polymerase 5'-RNA Capping Poly— Adenylation	150-VLSCLE**RVD**YDNAF-163 659-WIYYSD**RSD**LIGL-671
Rabies	Rhabdoviridae Lyssavirus	Pasteur / PV, SAD B19, ERA, Street, HEP-FLURY, vnukovo-32	**G** Spike Membrane Glycoprotein Precursor	276-LVNLHDF**RSD**EIEHLV-291
Human Parainfluenza type 3	Paramyxoviridae Paramyxovirinae Respirovirus	NIH 47885, Wash/1511/73, Aus/124854/74, Wash/641/79, Tex/545/80, Tex/9305/82, Tex/12677/83	**HN** Hemagglutinin— Neuraminidase	272-PKVDE**RSD**YASS-283

Table 1 (*continued*)

Virus	Virus Family	Strain	Virus Protein	B6RA/BNP
	Subfamily			Target Sequence
	Genus			
Measles	Paramyxoviridae Paramyxovirinae Morbillivirus	Edmonston, edmonston-zagreb, Halle, edmonston b, philadelphia-26, leningrad-16, Yamagata-1	**F** Fusion Membrane Glycoprotein Precursor	437-YPDAVYLH**RID**LGPPISL-454 450-PPISLE**RLD**VGTNLG-464
Measles	Paramyxoviridae Paramyxovirinae Morbillivirus	Edmonston, Rubeovax, Moraten, AIK-C, HU2, SE, Schwarz vaccine, CL, TT	**M** Viral Matrix Protein	186-VAFNLLVTL**RID**KAIGP-202
Human Respiratory Syncytial A	Paramyxoviridae Pneumovirinae Pneumovirus	A2	**L** RNA-directed RNA Polymerase Protein Kinase	917-Y**RGES**LLCSLIF-928
Human Respiratory Syncytial A / B	Paramyxoviridae Pneumovirinae Pneumovirus	A2, Long, subgroup B/strain 18537	**P** Phosphoprotein **L**/N-binding mRNA 5'-Capping and Polyadenylation	131-ITA**RLDRID**EKLSEIL-146
Marburg	Filoviridae Filovirus Marburg virus	Musoke, Popp	**NP** Nucleocapsid Major Nucleoprotein	558-PPPPLYAQEK**RQD**PIQHP-575
Marburg	Filoviridae Filovirus Marburg virus	Musoke	**L** RNA-directed RNA Polymerase mRNA 5'-Capping and Polyadenylation	1169-LLPYDCKEL**RLEG**S-1182 1763-ITKHDQ**RCEREES**SP-1777
Marburg	Filoviridae Filovirus Marburg virus	Musoke, Popp	**M/VP40** Viral Matrix Protein	262-MMKK**RGE**NSPVVYF-275
Human Hepatitis A	Picornaviridae Hepatovirus	HM-175 wild type, 18F, 24A, 43C, LA, MBB	**2C** Initiation of RNA Synthesis	1216-AMVT**RCE**PVVCYL-1228

Table 1 (continued)

Virus	Virus Family Subfamily Genus	Strain	Virus Protein	B6RA/BNP Target Sequence
Yellow Fever	Flaviviridae Flavivirus	17D, Pasteur 17D-204	**NS5** RNA-dependent RNA Polymerase	2638-IH**RLE**PVKCDTLL-2650 3148-SVLT**RLE**AWLT-3158
Dengue type 1	Flaviviridae Flavivirus	Singapore S275/90	**NS3** Protease NTP-Binding Helicase	2011-LMR**RGD**LPVWLSY-2023
Dengue type 2	Flaviviridae Flavivirus	Jamaica, 16681, PR159/S1, 16681-PDK53, New Guinea-C, Tonga 1974	**NS3** Protease NTP-Binding Helicase	2011-LMR**RGD**LPVWLAY-2023
Dengue type 3	Flaviviridae Flavivirus	—	**NS3** Protease NTP-Binding Helicase	2010-LMR**RGD**LPVWLAH-2022
Dengue type 4	Flaviviridae Flavivirus	—	**NS3** Protease NTP-Binding Helicase	2009-LMR**RGD**LPVWLSY-2021
West Nile	Flaviviridae Flavivirus	WN-NY99	**E/V3** Membrane— Associated Viral Envelope Glycoprotein	370-AHNDK**RAD**PAFVC-382
Kunjin	Flaviviridae Flavivirus	MRM61C	**E** Membrane— Associated Viral Envelope Glycoprotein	370-AHNDK**RAD**PSFVC-382
St. Louis Encephalitis	Flaviviridae Flavivirus	MS1-7	**E** Major Envelope Protein	368-AHNTK**RSD**PTFVC-380
Hepatitis C	Flaviviridae Hepacivirus	1, BK, J, Taiwan, Japanese, H77, HCV-1, H, JK1, JK5, HC-JT	**E2/NS1** Glycosylated Membrane Protein	646-WT**RGERCD**LEDRDR-659
Rubella	Togaviridae Rubivirus	Therien	**NSP1-2** Nonstructural Polyprotein 5'-Cap Methyltransferase Zn^{2+}-Cysteine Protease	494-CACAP**RCD**VPRERPSAP-510

Table 1 (*continued*)

Virus	Virus Family / Subfamily / Genus	Strain	Virus Protein	B6RA/BNP Target Sequence
Rubella	Togaviridae Rubivirus	Therien, HPV77 vaccine, RA27/3 vaccine	**C** Structural Polyprotein Nucleocapsid Protein	165-AVFY**RVD**LHFTNLGTPP-181
Human Corona	Coronaviridae Coronavirus	229E	**S/E2** Surface Spike Glycoprotein Precursor Aminopeptidase N-binding	94-FVYFNGTG**RGD**CKGFSSDV-112 257-SVINRL**RCD**QLSFDVP-272 636-ALRNSA**RLES**ADVSEML-652 1016-VTFVNIS**RSE**LQTIVP-1031 1099-LVDLKWLN**RVE**TYIKWP-1115
Marburg	Filoviridae Filovirus Marburg virus	Musoke, Popp	**VP30** Phosphorylated Nucleocapsid Protein	160-YLH**RSE**IGNWM-170
Marburg	Filoviridae Filovirus Marburg virus	Musoke, Popp	**VP24** Membrane-associated Structural Protein	197-FLVEVR**RID**IEPCC-210
Ebola	Filoviridae Filovirus Ebola virus Zaire	Mayinga, Zaire-95, Gabon-94	**NP** Nucleocapsid Major Nucleoprotein	103-GF**RFE**VKKRDGV-114 108-VKKRDGV**KRLEE**LLPAV-124
Ebola	Filoviridae Filovirus Ebola virus Zaire	Mayinga	**P/VP35** Polymerase Complex Protein (Minor Nucleoprotein)	292-PPVIHIRS**RGD**IPRAC-307
Borna Disease	Bornaviridae Bornavirus	He/80, He/80/FR, V, V/FR, H1766, No/98, CRNP5, CRP3A, CRP3B	**P/p23** Nucleocapsid Phosphorylated P-Protein	99-DISA**RIE**AGF-108 116-VETIQTAQ**RCD**HSDSIR-132
Borna Disease	Bornaviridae Bornavirus	He/80, He/80/FR, V, V/FR, H1766, CRNP5, CRP3A, CRP3B	**N/p40** Nucleocapsid Nucleic Acid-binding N-Protein	100-YLSTPVT**RGE**QTVV-113 339-YRRREIS**RGE**DGAELS-354
Hantaan	Bunyaviridae Hantavirus	76-118, 84Fli, A16	**M** Polyprotein Segment/ Glycosylated Membrane **G1** Protein	420-VNFVCQ**RVD**MDIVVYC-435
Hantaan	Bunyaviridae Hantavirus	R22	**M** Polyprotein Segment/ Glycosylated Membrane **G1** Protein	418-ISFICQ**RVD**MDIIVYC-433

Table 1 (*continued*)

Virus	Virus Family	Strain	Virus Protein	B6RA/BNP
	Subfamily			Target Sequence
	Genus			
Lassa	Arenaviridae Arenavirus Old World Arenaviruses	Josiah	**NP S Segment** Major Structural Nucleoprotein Nucleocapsid Component	113-VI**RTER**PLSAGVYM-126
Lassa	Arenaviridae Arenavirus Old World Arenaviruses	GA391 Nigeria	**NP S Segment** Major Structural Nucleoprotein Nucleocapsid Component	113-VT**RTER**PLSSGVYM-126
Human Rota group A	Reoviridae Rotavirus Rotavirus A Human Rotavirus A	KU	**VP4/VP5** Outer Layer Surface Protein Hemagglutinin Fusion Protein	336-FSVS**RYE**VIKENSYVYV-352 482-PIMNSVTV**RQD**LERQL-497 733-YGIT**RIE**ALNLI-744 760-PIIRN**RIE**QLILQC-773
Human Immunodeficiency type 1	Retroviridae Lentivirus	HIV-1 Reference Genome, HTLV-III/LAV, HXB2, BRU, PV22, RF/HAT	**Tat** *Trans*-activating Transcriptional Regulatory Protein	1-MEPVDP**RLE**PW-11 73-PTSQP**RGD**PTGP-84
Human Immunodeficiency type 1	Retroviridae Lentivirus	HXB3, BH10, Clone 12	**Tat** *Trans*-activating Transcriptional Regulatory Protein	1-MEPVDP**RLE**PW-11 73-PTSQS**RGD**PTGP-84
Human Immunodeficiency type 1	Retroviridae Lentivirus	HIV-1 Reference Genome, HTLV-III/LAV, HXB2, BRU, PV22, RF/HAT, BH10, Clone 12	**Vif (Sor)** Viral Infectivity Factor Accessory Protein	129-VSP**RCE**YQA-137
Human Immunodeficiency type 1	Retroviridae Lentivirus	HIV-1 Reference Genome, HTLV-III/LAV, HXB2, BRU	**Nef/p27** Negative Factor Anti-apoptotic Accessory Protein	13-WPTVRERMR**RAE**PAA-27 100-LIHSQR**RQD**ILDLWIY-115

[Cu(OH)₂] precipitated. Solution B: 50 mL of an at 80 °C saturated solution of 1-[3-hydroxy-5-(hydroxymethyl)-2-methyl-4-pyridinyl]-2,8,9-trioxaadamantane-3,5,7-triol (bananin) in 5 M sodium hydroxide solution. Freshly prepared suspension A was mixed with solution B and was cooled at +4 °C for 2 h. The light blue precipitate was vacuum filtered and dried over anhydrous calcium chloride (CaCl₂) in a vacuum desiccator. Yield: dark blue amorphous powder (*SP-4-1*)-bis[1-[3-hydroxy-5-(hydroxymethyl)-2-methyl-4-pyridinyl]-2,8,9-trioxaadamantane - 3,5,7 - triolato(1-)-$O^2,O^{3'}$]copper [bananin copper complex, bis (bananinato)copper, bisBNcopper].

Qualitative preparation of amorphous (*T-4*)-bis[1-[3-hydroxy-5-(hydroxymethyl)-2-methyl-4-pyridinyl]-2,8,9-trioxaadamantane-3,5,7-triolato(1-)-$O^2,O^{3'}$]zinc [bananin zinc complex, bis(bananinato)zinc, bisBNzinc]

Solution A: a saturated (room temperature θ = 20 °C) solution of anhydrous zinc chloride (ZnCl₂) in 10 mL of water. Solution B: 50 mL of an at 80° C saturated solution of 1-[3-hydroxy-5-(hydroxymethyl)-2-methyl-4-pyridinyl]-2,8,9-trioxaadamantane-3,5,7-triol (bananin) in 5 M sodium hydroxide solution. Freshly prepared solution A was mixed with solution B and was cooled at +4° C for 2 h. The white precipitate was vacuum filtered and dried over anhydrous calcium chloride (CaCl₂) in a vacuum desiccator. Yield: white amorphous powder (*T-4*)-bis[1-[3-hydroxy-5-(hydroxymethyl)-2-methyl-4-pyridinyl]-2,8,9-trioxaadamantane-3,5,7-triolato(1-)-$O^2,O^{3'}$]zinc [bananin zinc complex, bis(bananinato)zinc, bisBNzinc].

Acknowledgements

References and Notes

1. Woodward, R. B. *Pure Appl. Chem.* **1964**, *9*, 49.

2. Tsuda, K.; Ikuma, S.; Kawamura, M.; Tachikawa, R.; Sakai, K.; Tamura, C.; Amakasu, O. *Chem. Pharm. Bull.* **1964**, *12*, 1357.

3. Goto, T.; Kishi, Y.; Takahashi, S.; Hirata, Y. *Tetrahedron* **1965**, *21*, 2059.

4. Wagner, H.; Fischer, M.; Lotter, H. *Z. Naturforsch* **1985**, *40b*, 1226.

5. Wagner, H.; Lotter, H.; Fischer, M. *Helv. Chim. Acta* **1986**, *69*, 359.

6. Schiff, H. *Ann. Chem. Pharm.* **1865**, *3* (Suppl.), 343.

7. Tryfiates, G. P.; Gannett, P. M.; Bishop, R. E.; Shastri, P. K.; Ammons, J. R.; Arbogast, J. G. *Cancer Res.* **1996**, *56*, 3670.

8. Kesel, A. J.; Urban, S.; Oberthür, W. *Tetrahedron* **1996**, *52*, 14787.

9. Kesel, A. J.; Polborn, K.; Gürtler, L.; Klinkert, W. E. F.; Modolell, M.; Oberthür, W. *J. Cancer Res. Clin. Oncol.* **1998**, *124* (Suppl.), S32.

10. Kesel, A. J.; Sonnenbichler, I.; Polborn, K.; Gurtler, L.;

11. Kesel, A. J.; Sonnenbichler, I.; Polborn, K.; Gürtler, L.; Klinkert, W. E. F.; Modolell, M.; Nüssler, A. K.; Oberthür, W. *Bioorg. Med. Chem.* **1999**, *7*, 359.

12. Kesel, A. J. *Biochem. Biophys. Res. Comm* **2003**, *300*, 793.

13. Hanna, M. C.; Turner, A. J.; Kirkness, E. F. *J. Biol. Chem.* **1997**, *272*, 10756.

14. Zhang, Z.; McCormick, D. B. *Proc. Natl. Acad. Sci. U.S.A.* **1991**, *88*, 10407.

15. McCormick, D. B.; Chen, H. *J. Nutr.* **1999**, *129*, 325.

16. Li, M.-H.; Kwok, F.; Chang, W.-R.; Lau, C.-K.; Zhang, J.-P.; Lo, S. C. L.; Jiang, T.; Liang, D.-C. *J. Biol. Chem.* **2002**, *277*, 46385.

17. Rice, W. G.; Schaeffer, C. A.; Harten, B.; Villinger, F.; South, T. L.; Summers, M. F.; Henderson, L. E.; Bess, J. W., jr; Arthur, L. O.; McDougal, J. S.; Orloff, S. L.; Mendeleyev, J.; Kun, E. *Nature (London)* **1993**, *361*, 473.

18. Chuang, A. J.; Killam, K. M., jr; Chuang, R. Y.; Rice, W. G.; Schaeffer, C. A.; Mendeleyev, J.; Kun, E. *FEBS Lett.* **1993**, *326*, 140.

19. Rice, W. G.; Schaeffer, C. A.; Graham, L.; Bu, M.; McDougal, J. S.; Orloff, S. L.; Villinger, F.; Young, M.; Oroszlan, S.; Fesen, M. R.; Pommier, Y.; Mendeleyev, J.; Kun, E. *Proc. Natl. Acad. Sci. U.S.A.* **1993**, *90*, 9721.

20. Wondrak, E. M.; Sakaguchi, K.; Rice, W. G.; Kun, E.; Kimmel, A. R.; Louis, J. M. *J. Biol. Chem.* **1994**, *269*, 21948.

21. Rice, W. G.; Supko, J. G.; Malspeis, L.; Buckheit, R. W., jr; Clanton, D.; Bu, M.; Graham, L.; Schaeffer, C. A.; Turpin, J. A.; Domagala, J.; Gogliotti, R.; Bader, J. P.; Halliday, S. M.; Coren, L.; Sowder, R. C.; Arthur, L. O.; Henderson, L. E. *Science* **1995**, *270*, 1194.

22. Rice, W. G.; Turpin, J. A. *Rev. Med. Virol.* **1996**, *6*, 187.

23. Turpin, J. A.; Terpening, S. J.; Schaeffer, C. A.; Yu, G.; Glover, C. J.; Felsted, R. L.; Sausville, E. A.; Rice, W. G. *J. Virol.* **1996**, *70*, 6180.

24. Rice, W. G.; Turpin, J. A.; Schaeffer, C. A.; Graham, L.; Clanton, D.; Buckheit, R. W., jr; Zaharevitz, D.; Summers, M. F.; Wallqvist, A.; Covell, D. G. *J. Med. Chem.* **1996**, *39*, 3606.

25. Rice, W. G.; Baker, D. C.; Schaeffer, C. A.; Graham, L.; Bu, M.; Terpening, S.; Clanton, D.; Schultz, R.; Bader, J. P.; Buckheit, R. W., jr; Field, L.; Singh, P. K.; Turpin, J. A. *Antimicrob. Agents Chemother.* **1997**, *41*, 419.

26. Rice, W. G.; Turpin, J. A.; Huang, M.; Clanton, D.; Buckheit, R. W., jr; Covell, D. G.; Wallqvist, A.; McDonnell, N. B.; De Guzman, R. N.; Summers, M. F.; Zalkow, L.; Bader, J. P.; Haugwitz, R. D.; Sausville, E. A. *Nat. Med.* **1997**, *3*, 341.

27. Domagala, J. M.; Bader, J. P.; Gogliotti, R. D.; Sanchez, J. P.; Stier, M. A.; Song, Y.; Prasad, J. V.; Tummino, P. J.; Scholten, J.; Harvey, P.; Holler, T.; Gracheck, S.; Hupe, D.; Rice, W. G.; Schultz, R. *Bioorg. Med. Chem.* **1997**, *5*, 569.

28. McDonnell, N. B.; De Guzman, R. N.; Rice, W. G.; Turpin, J. A.; Summers, M. F. *J. Med. Chem.* **1997**, *40*, 1969.

29. Huang, M.; Maynard, A.; Turpin, J. A.; Graham, L.; Janini, G. M.; Covell, D. G.; Rice, W. G. *J. Med. Chem.* **1998**, *41*, 1371.

30. Maynard, A. T.; Huang, M.; Rice, W. G.; Covell, D. G. *Proc. Natl. Acad. Sci. U.S.A.* **1998**, *95*, 11578.

31. Turpin, J. A.; Song, Y.; Inman, J. K.; Huang, M.; Wallqvist, A.; Maynard, A.; Covell, D. G.; Rice, W. G.; Appella, E. *J. Med. Chem.* **1999**, *42*, 67.

32. Basrur, V.; Song, Y.; Mazur, S. J.; Higashimoto, Y.; Turpin, J. A.; Rice, W. G.; Inman, J. K.; Appella, E. *J. Biol. Chem.* **2000**, *275*, 14890.

33. Goel, A.; Mazur, S. J.; Fattah, R. J.; Hartman, T. L.; Turpin, J. A.; Huang, M.; Rice, W. G.; Appella, E.; Inman, J. K. *Bioorg. Med. Chem. Lett.* **2002**, *12*, 767.

34. Schito, M. L.; Goel, A.; Song, Y.; Inman, J. K.; Fattah, R. J.; Rice, W. G.; Turpin, J. A.; Sher, A.; Appella, E. *AIDS Res. Hum. Retroviruses* **2003**, *19*, 91.

35. Mayasundari, A.; Rice, W. G.; Diminnie, J. B.; Baker, D. C. *Bioorg. Med. Chem.* **2003**, *11*, 3215.

36. *Atlas of Protein and Genomic Sequences*®, Version 4.0; National Biomedical Research Foundation, Washington, DC, USA, June 30, 1994. Martinsried Institute for Protein Sequences (MIPS), Max-Planck-Institute for Biochemistry, Martinsried, Germany.

37. Medline/PubMed. National Center for Biotechnology Information (NCBI), National Library of Medcine (NLM): 8600 Rockville Pike, Bethesda, MD 20894, USA. Internet address: http://www.ncbi.nlm.nih.gov/entrez/query.fcgi.

38. Hirsch, M. S.; Kaplan, J. C.; D'Aquila, R. T. In: Fields Virology; Fields, B. N.; Knipe, D. M.; Howley, P. M.; Chanock, R. M.; Melnick, J. L.; Monath, T. P.; Roizman, B.; Straus, S. E., Eds.; third ed., Lippincott-Raven: Philadelphia, 1996; pp. 431–466.